

Original software publication



# UAVradio: Radio link path loss estimation for UAVs

Daniel Aláez<sup>a,b,\*</sup>, Mikel Celaya-Echarri<sup>a,b</sup>, Leyre Azpilicueta<sup>b,c</sup>, Jesús Villadangos<sup>a,b</sup>

<sup>a</sup> *Mathematical Engineering and Computer Science Department, Public University of Navarre (UPNA), Pamplona, 31006, Spain*

<sup>b</sup> *Institute of Smart Cities, Pamplona, 31006, Spain*

<sup>c</sup> *Electric, Electronic and Communications Department, Public University of Navarre (UPNA), Pamplona, 31006, Spain*

## ARTICLE INFO

### Keywords:

UAV  
Radio  
Path loss  
Simulation  
Model  
Communications

## ABSTRACT

The UAVRadio Python module is a comprehensive toolkit designed to facilitate the analysis and prediction of radio signal path loss in Unmanned Aerial Vehicle (UAV) communication scenarios. The module encompasses a range of path loss models referenced from established literature, offering users a powerful and flexible framework for estimating signal attenuation in different UAV communication links. It is a versatile and modular tool that enables simple integration for optimizing UAV communication systems and ensuring reliable wireless connectivity in a variety of operational scenarios. The utility of this package is demonstrated through two relevant examples: an experimentally fit model comparison with other implemented models, and a UAV digital twin implementation example comparing different available models and frequencies. The examples are provided in the code repository along with comprehensive documentation.

## Code metadata

Current code version	v0.1
Permanent link to code/repository used for this code version	<a href="https://github.com/ElsevierSoftwareX/SOFTX-D-23-00731">https://github.com/ElsevierSoftwareX/SOFTX-D-23-00731</a>
Permanent link to Reproducible Capsule	
Legal Code License	MIT License
Code versioning system used	none
Software code languages, tools, and services used	Python
Compilation requirements, operating environments & dependencies	pip or conda, matplotlib, math, cmath, numpy
If available Link to developer documentation/manual	<a href="http://51.91.59.240/uav-radio">http://51.91.59.240/uav-radio</a>
Support email for questions	<a href="mailto:daniel.alaez@unavarra.es">daniel.alaez@unavarra.es</a>

## 1. Motivation and significance

With the rapid deployment of Unmanned Aerial Vehicles (UAVs) for both civil and military applications in the last few years, the analysis of wireless communications within UAV links has become crucial. In a UAV wireless communication link, the transmission medium is the radio channel between the transmitter and the receiver, where the signal can get to the receiver via different propagation paths (i.e., multipath components), which are affected by the obstacles in the environment, such as houses, mountains, trees, etc. for outdoor environments. Furthermore, UAV communication has its own distinctive channel characteristics compared to the widely used cellular or satellite systems, in which the most unique features are the highly dynamic communication due to UAV velocity, the excessive spatial and

temporal variations induced by the non-stationary channels, and the airframe shadowing caused by the structural design and rotation of the UAV [1,2]. Therefore, it is important to consider accurate propagation models to estimate the received signal within different scenarios and communication links [3].

### 1.1. Related works of UAVs communications

Several high-quality survey and tutorial articles on UAV communications have recently been published. The authors of [4] provide an overview of UAV-aided wireless communications, where channel characteristics, networking architecture, and key design considerations for UAV communications are presented. A survey on channel modeling

\* Corresponding author at: Mathematical Engineering and Computer Science Department, Public University of Navarre (UPNA), Pamplona, 31006, Spain.  
E-mail address: [daniel.alaez@unavarra.es](mailto:daniel.alaez@unavarra.es) (D. Aláez).

for UAV communications is provided in [2], where different measurement approaches and various channel characterizations are presented for real-world UAV communications scenarios. The same authors focused in [1] on air-to-ground (AG) propagation channel modeling for UAV, where they present large- and small-scale fading, multiple-input-multiple-output (MIMO) channel characteristics and simulations. Furthermore, with the recent development of UAV communications for B5G systems, the authors in [5] provide the fundamentals of B5G UAV communications, including the channel model for two typical scenarios (i.e., UAV-assisted wireless communications and cellular-connected UAV). In [6], an exhaustive survey on UAV communication in 5G and B5G wireless networks is presented. Furthermore, the advantages, challenges, and promising technologies for cellular-connected UAVs are summarized in [7]. The authors of [8] provided key guidelines for analyzing, designing, and optimizing UAV-based wireless communication systems. Finally, the authors of [9] analyzed essential challenges for the deployment of mmWave-enabled UAV relays, and a complete work presented in [10] provides a comprehensive survey on mmWave beamforming-enabled UAV communications and networking, where an overview on relevant mmWave channel modeling approaches is provided. In summary, all the presented works highlight the importance of the propagation channel consideration to estimate the signal losses in the UAV communication link for the corresponding application.

### 1.2. Our contribution

In this regard, with the aim of facilitating the analysis and prediction of radio signal path loss in UAV communication scenarios, this work has developed a UAVRadio Python module as a comprehensive toolkit that allows considering the proper path loss model according to the scenario and analysis of UAV links. The primary aim of this module is to provide engineers, researchers, and enthusiasts in the field of UAV communications with a robust set of Python functions that enable accurate and efficient radio signal path loss predictions. This capability is essential for various applications, including but not limited to:

1. **Drone Communication Planning:** UAVs often rely on wireless communication for control, telemetry, and data transmission. Accurate path loss estimation is crucial for planning communication range and reliability.
2. **Environmental Analysis:** Different environments, such as urban, rural, and hilly terrain, can significantly affect signal propagation. This module allows users to model and assess path loss under diverse conditions and scenarios.
3. **Frequency Selection:** For optimal performance, UAV communication systems may operate at various frequencies. This module helps to select suitable frequencies by predicting path loss characteristics.

The Radio Link Path Loss Estimation for UAVs module includes the following key features:

1. **Implementation of multiple path loss models:** The module offers a selection of several well-established path loss models for UAV communications, including free space path loss, log-distance path loss, two-ray path loss, dual slope path loss, or path loss as a function of the elevation angle, among others. Users can choose the model that best suits their specific UAV communication scenario.
2. **Environmental considerations:** Some path loss models take into account environmental factors such as terrain type, foliage intensity, and water bodies. These considerations enhance the accuracy of path loss predictions.
3. **Conversion utilities:** The module provides methods for converting between 2D and 3D positions, calculating distances, and performing coordinate transformations. These utilities assist users in preparing input data for path loss estimation.

4. **Contour plot generation:** Users can visualize path loss variation across a specified area by generating contour plots centered around transmitter coordinates. The obtained data is three-dimensional, but to facilitate the results analysis, the contour plots can be obtained in 2D planes, which can be horizontal (XY) or vertical (XZ) plots. These results can help to understand the signal strength distribution in the UAV communication region.
5. **Customization and extensibility:** The module allows users to customize the parameters within the path loss models and easily extend it with new models as needed. The software is currently in use for multiple internal research projects at Universidad Pública de Navarra, so continuous software updates are expected with new functionalities and more models based on future literature studies.

A summary diagram of all currently available methods is shown in Fig. 1.

## 2. Software description

Currently, this module exclusively supports AG communications, which is the most common scenario for communications between an airborne UAV and the Ground Control Station (GCS). This configuration allows for the estimation of key parameters, including radio signal characteristics and telemetry data. A common AG propagation scenario is shown in Fig. 2 in the presence of terrestrial obstacles which are also commonly referred as scatterers. In the figure,  $h_{GCS}$ ,  $h_{UAV}$  represents the height of the GCS and the UAV above the ground, respectively,  $d$  is the slant range between the UAV antennas and the GCS,  $d_H$  is the horizontal distance between the UAV and GCS,  $r_1$  and  $r_2$  are the ground incident and reflected components path lengths, respectively, and  $\theta$  is the elevation angle between the GCS and UAV antennas.

As the number of models documented in the literature increases and their utility is validated, we intend to incorporate additional radio models capable of estimating air-to-air (AA) communications. A brief explanation of the current AG models included in the UAVRadio module is provided in the following subsections.

### 2.1. Free Space Path Loss model

The Free Space Path Loss propagation model can be used to estimate the line-of-sight (LOS) path loss in a free space environment. The model does not consider any objects in the scenario; thus, it can only be used with unobstructed clear path between the transmitter and the receiver. It is determined as follows [3]:

$$PL \text{ [dB]} = 20 \log_{10} \left( \frac{4\pi d}{\lambda} \right), \quad (1)$$

where  $d$  is the distance between TX and RX; and  $\lambda$  is the wavelength, (see Fig. 2 for reference).

### 2.2. Log-distance Path Loss model

The Log-distance Path Loss model is an extension of the Free Space Path Loss model that can be used to predict propagation loss for a wide range of environments. It can be calculated using the following formula [3]:

$$PL \text{ [dB]} = PL_0 + 10n \log_{10}(d/d_0) + X_\sigma, \quad (2)$$

where  $d$  is the distance between TX and RX;  $d_0$  is the reference distance, usually considered as  $d_0 = 1$  m,  $PL_0 = 10 * \log_{10} \left[ \frac{4\pi d_0}{\lambda} \right]$ ;  $n$  is the path loss exponent;  $\lambda$  is the wavelength; and  $X_\sigma \approx N(0, \sigma^2)$  is a random variable which presents the variations in the Free Space Path Loss model, following a normal distribution with standard deviation  $\sigma$ . The value of the path loss exponent (parameter  $n$ ) depends on the specific propagation environment and determines how the scatterers are present in the scenario. Its values are normally in the range of

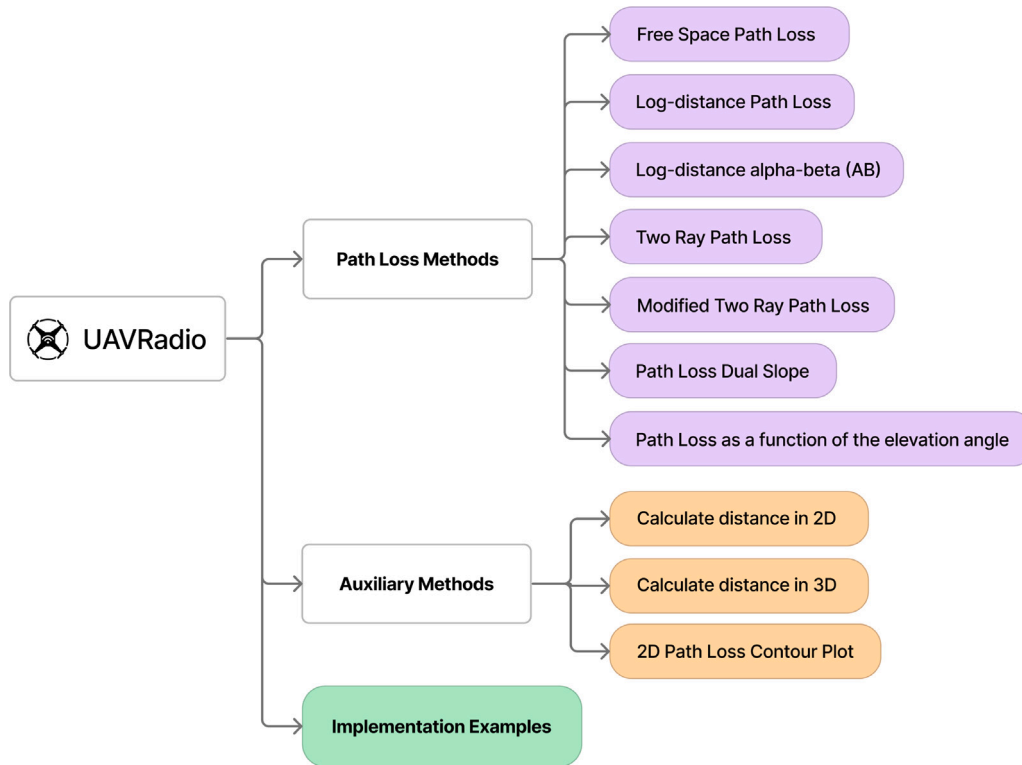


Fig. 1. UAVRadio Python package diagram overview.

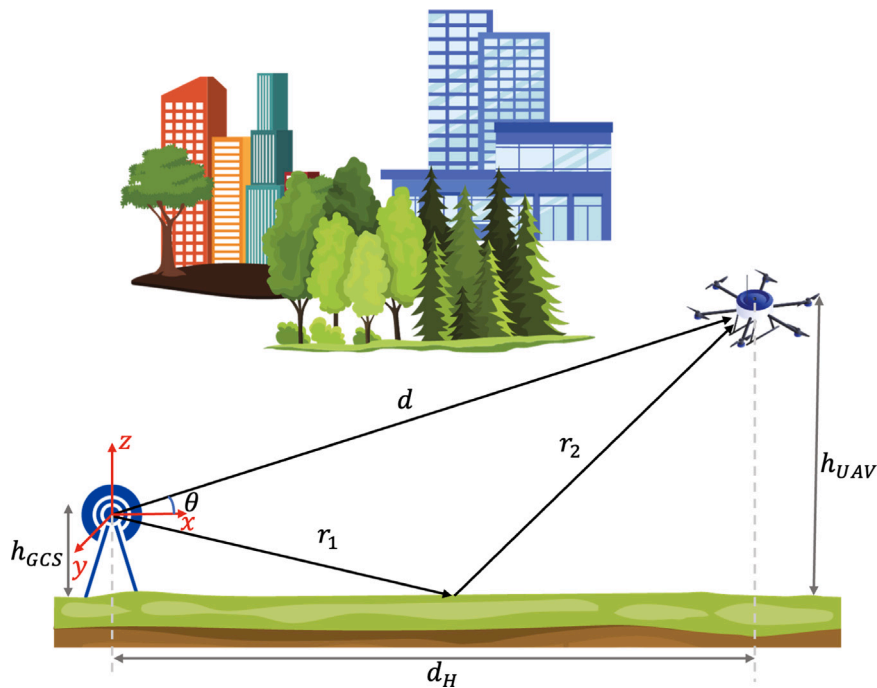


Fig. 2. A typical AG propagation scenario with a UAV.

2 to 4 (where 2 is for propagation in free space, and 4 is for lossy environments). In some environments, such as buildings, stadiums and other indoor environments, the path loss exponent can reach values in the range of 4 to 6 [11].

A summary of all preconfigured setups considered for AG communications for different scenarios based on these parameters is shown in Table 2.

### 2.3. Log-distance Alpha-Beta (AB) model

Another Path Loss model used in the literature for AG communications is the Alpha-Beta (AB) model or floating intercept (FI). This model is similar to (2), but the free space path loss at the reference distance  $PL_0$  is eliminated and the model is dependent on two parameters represented as  $\alpha$  and  $\beta$ , where  $\alpha$  is the slope and  $\beta$  represents the

**Table 1**  
Log-distance Alpha-Beta model preconfigured cases.

Scenario	UAV height (m)	$\alpha$	$\beta$ (dB)	$\sigma$ (dB)	Ref.
Lightly hilly rural	1.5	3.7	-1.3	7.7	[12]
	15	2.9	7.4	6.2	
	30	2.5	20.4	5.2	
	60	2.1	32.8	4.4	
	120	2.0	35.3	3.4	

intercept. The model is determined as follows:

$$PL \text{ [dB]} = \alpha 10 \log_{10}(d) + \beta + X_{\sigma}, \quad (3)$$

where  $d$  is the distance between TX and RX;  $\alpha$  is the path loss exponent;  $\beta$  is the intercept point with the line  $d = 1\text{m}$ ; and  $X_{\sigma} \approx N(0, \sigma^2)$  is a random variable representing the variations of the path loss.

The cases shown in Table 1 have been extracted from the literature and are ready to use in the model.

#### 2.4. Path loss dual slope model

The two path loss models presented before are based on a single slope. The use of these models is recommended in areas where the characteristics of the channel do not change drastically. However, in some scenarios with predominant non-line-of-sight (NLOS) conditions and complex geometries, the single-slope models can have larger errors. In such cases, a Dual Slope Path Loss model can be used, which is similar to the AB model, but has two different slopes for different link distance ranges, and can be represented as follows [19]:

$$PL \text{ [dB]} = \begin{cases} PL_{d_0} + 10\gamma_1 \cdot \log_{10} \frac{d}{d_0}, & d < d_b \\ PL_{d_0} + 10\gamma_1 \cdot \log_{10} \frac{d_b}{d_0} + 10\gamma_2 \cdot \log_{10} \frac{d}{d_0}, & d \geq d_b \end{cases} \quad (4)$$

where  $d_0$  is the reference distance;  $d_b$  is the break distance; and  $\gamma_1$  and  $\gamma_2$  are the path loss exponents.

The available setups from the literature are shown in Table 3.

#### 2.5. Path loss as a function of the elevation angle

In case the elevation angle is preferred to calculate the link losses in the AG communication scenario, Ref. [1] describes the path loss as a function of the elevation angle  $\theta$  between the UAV and GCS, which is given as follows:

$$PL = 20 \log_{10} \left( \frac{\Delta h}{\sin \theta} \right) + 20 \log_{10}(f_{\text{MHz}}) - 27.55, \quad (5)$$

where  $\Delta h = h_{UAV} - h_{GCS}$  is the difference between the height of the UAV and the height of the GCS in meters;  $f$  is the frequency in MHz;  $\theta$  is the elevation angle between the UAV and the GS; and  $\frac{\Delta h}{\sin \theta}$  is the link distance expressed as a function of the elevation angle (see Fig. 2 for reference). The argument  $\frac{\Delta h}{\sin \theta}$  is simply the link distance expressed as a function of the elevation angle.

#### 2.6. Two Ray Path Loss Model

In the case of the Two Ray Path Loss Model, the variation of path loss with distance has distinctive peaks due to destructive summation of the dominant and surface-reflected component. This model considers the assumption that  $r_1 + r_2 \approx d$  (which is the typical AG scenario shown in Fig. 2). It can be determined as follows [3]:

$$PL \text{ [dB]} = -10 \log_{10} \left\{ \left( \frac{\lambda}{4\pi d} \right)^2 \left[ 2 \sin \left( \frac{2\pi h_{GCS} h_{UAV}}{\lambda d} \right) \right]^2 \right\}, \quad (6)$$

where  $d$  is the distance between TX and RX;  $\lambda$  is the wavelength;  $h_{GCS}$  is the TX height above ground; and  $h_{UAV}$  is the RX height above ground (see Fig. 2 for reference).

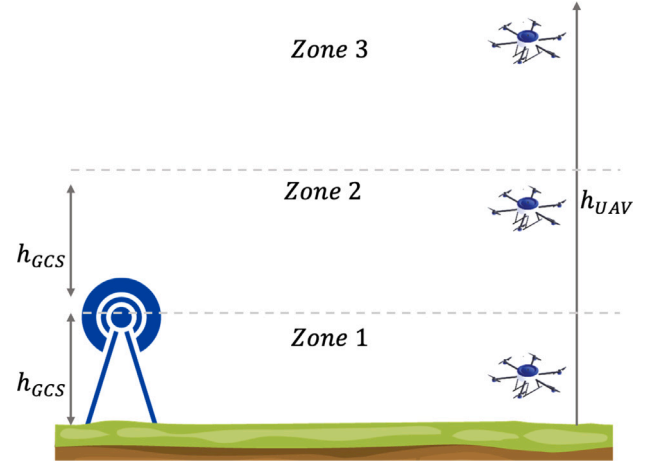


Fig. 3. Different zones considered for the Modified Two Ray Path Loss model.

#### 2.7. Modified Two Ray Path Loss Model

For different scenarios where the UAV can be significantly higher than the GCS, the Modified Two Ray Path Loss model is proposed in [20]. This model is based on the two-ray transmission equation (Eq. (6)) but it does not consider the assumption typically used for cellular ground coverage, in particular  $r_1 + r_2 \approx d$  is not valid. Based on this, it considers three different zones, depending on the heights of the UAV and the GCS. Fig. 3 presents the three different zones, which are described as follows:

1. Zone 1 ( $h_{UAV} \leq h_{GCS}$ ): drone height approximately lower than the GCS height.
2. Zone 2 ( $h_{GCS} < h_{UAV} \leq 2h_{GCS}$ ): drone height over GCS height and below two times the GCS height.
3. Zone 3 ( $h_{UAV} > 2h_{GCS}$ ): drone height more than twice the GCS height.

The formulation proposed in the literature [20] can be expressed in terms of PL as follows:

$$PL \text{ [dB]} = 20 \log_{10} \left( \frac{4\pi}{\lambda} \right) - 10\gamma(h) \log_{10} \left( \left| \frac{G_l(h)}{d} + \frac{RG_r(h)}{r_1 + r_2} \right| \right). \quad (7)$$

where

$$d = d_H \sqrt{1 + \frac{(h_{GCS} - h_{UAV})^2}{d_H^2}}, \quad (8)$$

$$r_1 = \sqrt{h_{GCS}^2 + \frac{(d_H h_{GCS})^2}{(h_{GCS} + h_{UAV})^2}}, \quad (9)$$

and

$$r_2 = \sqrt{h_{UAV}^2 + \left( d_H - \frac{d_H h_{GCS}}{(h_{GCS} + h_{UAV})} \right)^2}. \quad (10)$$

The direct path coefficient is specified by  $G_l(h)$ ; the reflected path by  $G_r(h)$ ; the height-dependent propagation coefficient by  $\gamma(h)$ ; and the ground reflection coefficient  $R$ . The parameters  $d$ ,  $r_1$ ,  $r_2$ ,  $h_{GCS}$ ,  $h_{UAV}$  and  $d_H$  can be obtained from the geometry presented in Fig. 2. The cases shown in Table 4 have been extracted from the literature and are ready to use in the model.

### 3. Illustrative examples

The best way to illustrate the utility of this module is with a few examples. First, we will present a comparison of all the presented

**Table 2**  
Log-distance Path Loss model preconfigured cases.

Scenarios	$n$	$\sigma$ (dB)	Ref.
Open field	2.0	–	[13]
Urban/Rural	4.1	5.2	[14]
Urban (Freq = 0.9–1.2 GHz)	1.7	2.6	
Urban (Freq = 5.03–5.091 GHz)	2.0	3.2	
Suburban (Freq = 0.9–1.2 GHz)	1.7	3.1	[15]
Suburban (Freq = 5.03–5.091 GHz)	1.5	2.9	
Open field Freq = 3.1–5.3 GHz $v = 0$ mph	$h_{GCS} = 1.5$ m (in foliage) $h_{GCS} = 1.5$ m (no foliage) $h_{GCS} = 7$ cm (from ground)	2.6 2.5 2.9	3.3 3.0 2.7
Open field Freq = 3.1–5.3 GHz $v = 20$ mph	$h_{GCS} = 1.5$ m (in foliage) $h_{GCS} = 1.5$ m (no foliage) $h_{GCS} = 7$ cm (from ground)	2.6 2.6 2.9	4.0 3.9 3.4 [16]
Suburban Freq = 3.1–5.3 GHz $v = 0$ mph	$h_{GCS} = 1.5$ m (in foliage) $h_{GCS} = 1.5$ m (no foliage) $h_{GCS} = 7$ cm (from ground)	2.7 2.6 3.0	4.8 4.3 4.8
Suburban Freq = 3.1–5.3 GHz $v = 20$ mph	$h_{GCS} = 1.5$ m (in foliage) $h_{GCS} = 1.5$ m (no foliage) $h_{GCS} = 7$ cm (from ground)	2.8 2.6 2.9	5.3 4.9 4.7
Hilly terrain with mountain ridge (Freq = 0.9–1.2 GHz)	1.6	3.5	
Hilly terrain with mountain ridge (Freq = 5.03–5.091 GHz)	1.7	2.8	
Dry, hilly terrain (Freq = 0.9–1.2 GHz)	1.3	3.9	
Dry, hilly terrain (Freq = 5.03–5.091 GHz)	1.0	2.2	[17]
Very mountainous terrain (Freq = 0.9–1.2 GHz)	1.6	3.5	
Very mountainous terrain (Freq = 5.03–5.091 GHz)	1.7	2.8	
Over fresh water (Freq = 0.9–1.2 GHz)	1.9	3.8	
Over fresh water (Freq = 5.03–5.091 GHz)	1.9	3.1	
Over sea (Freq = 0.9–1.2 GHz)	1.9	4.2	[18]
Over sea (Freq = 5.03–5.091 GHz)	1.5	2.6	

**Table 3**  
Dual Slope Path Loss model preconfigured cases.

Scenario	UAV height (m)	$\gamma_1$	$\gamma_2$	$\psi$ (dB)	Ref.
Ensemble of containers	20	0.74	2.29	5.5	[19]
	30			3.9	

**Table 4**  
Modified Two Ray Path Loss model parameters based on bibliography. The height  $h$  is in meters [20].

Scenarios	$G_t(h)$	$G_r(h)$	$\gamma(h)$	$R$
Zone 1 ( $h_{GCS} \leq 30$ )	15	5	3.5	–1
Zone 2 ( $30 < h_{GCS} \leq 60$ )	7	7	2.75	–1
Zone 3 ( $h_{GCS} > 60$ )	0	3.5	2	–1

models within a real scenario from the bibliography, to highlight the different available options and demonstrate the relevance of a correct model selection. Next, we will integrate this framework with an open-source UAV digital twin to extend its capabilities for radio signal path loss estimation, showing the impact of considering different frequencies in the available models, which could be of great interest when planning a mission.

### 3.1. Model plot comparison

In the first example, we have considered the real scenario presented in [12], where experimental measurements were conducted on live Long Term Evolution (LTE) networks in the 800 MHz frequency band, using a commercial UAV, in a slightly hilly area in Denmark. Field measurements were carried out at different heights: 1.5, 15, 30, 60 and 120 m above ground level, to obtain the fitted path loss models [12]. In order to analyze the radio channel model in UAV communications in this scenario, all models previously presented in Section 2 have been used and compared with the fitted path loss models, to show the capabilities of the presented software. The average height of the

LTE transmitter is not disclosed in [12], so an arbitrary height of  $h_t = 15$  m has been selected for the models that require it. With these considerations, the best matching models from the implemented library have been selected for fair comparison, which are the following:

- Log-distance Path Loss model:  $n = 2.01$ , open-field setting based on [13].
- Two-ray Path Loss model:  $h_t = 15$  m,  $h_r = [1.5, 15, 30, 60, 120]$  m.
- Modified Two-ray Path Loss model:  $h_t = 15$  m,  $h_r = [1.5, 15, 30, 60, 120]$  m.
- Dual Slope Path Loss model:  $h_r = 30$  m for all cases, since it is the only available preset as presented in [19].

The path loss as a function of the Elevation Angle described in Section 2.5 has not been included in this analysis, since it is essentially a modified model to express the distance in terms of height and elevation angle. However, this model could also be used depending on the user's requirements or preferences to visualize the results.

For the experiment, we chose a set of 20 linearly spaced points ranging from 0 to 200 m. The limited number of samples was intentionally chosen to enhance the clarity of visualizing multiple models within a single figure. The results are presented in Fig. 4, where Fig. 4(a) contains an overlap of the models fitted in the literature for each receiver height, and the remaining plots (Figs. 4(b)–(f)) compare the available models at each analyzed height and the fitted path loss model, which is presented by a black solid line with a circle marker for each height plot.

As can be seen in the figure, each model estimates losses differently, highlighting the importance of considering a suitable model for the specific case under analysis. The library of implemented models permits to compare different cases depending on the scenario, frequency, height, and the analyzed application, where the user can select the best model for each specific case. In order to show the differences between the implemented models and the fitted model in [12], Fig. 5 shows the mean absolute error and standard deviation for each model at the corresponding height (relative to the fitted model), showing the importance of selecting an appropriate model for each specific case, so

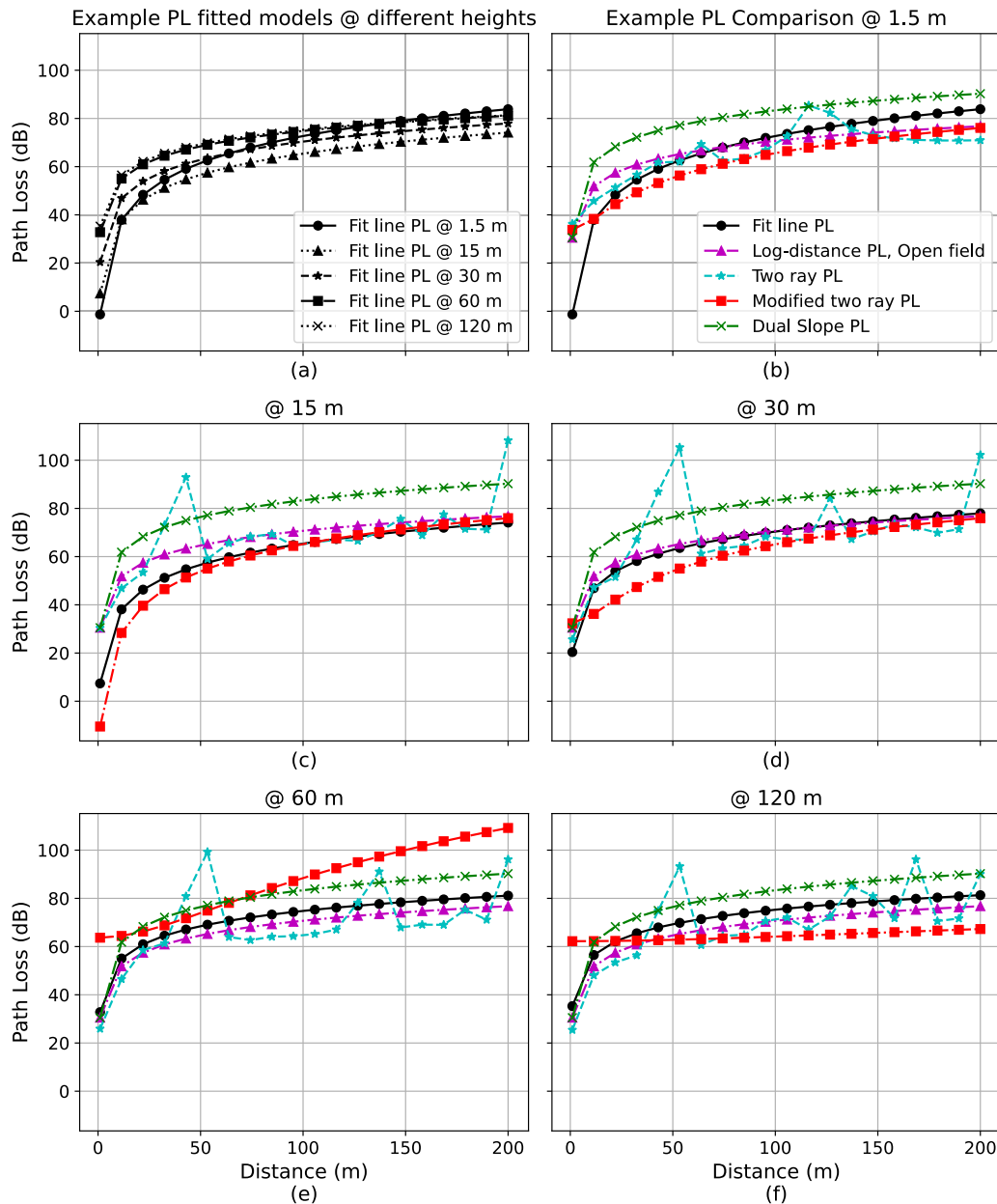


Fig. 4. Path Loss comparison at different heights between the fitted model from [12] and the implemented models, (a) PL fitted models at different heights, (b) 1.5 m, (c) 15 m, (d) 30 m, (e) 60 m, (f) 120 m.

that the mean absolute error is smaller when compared with field data measurements.

### 3.2. Open source UAV digital twin integration

In the following example, a basic Robot Operating System,<sup>1</sup> (ROS) integration will be shown. For simplicity, we recommend installing Intelligent Quads' *iq\_sim*<sup>2</sup> since it includes many pre-configured simulation environments for UAV testing with Ardupilot<sup>3</sup>. Although this example has been tested with the *multidrone* setup, the code should work with any other environment. An example of the proposed example setup is shown in Fig. 6.

This experiment aims to continuously estimate the radio signal path loss between a flying quadcopter (namely *drone1*), and the GCS located at the origin of coordinates in the Gazebo<sup>4</sup> world. The structure of the code example is as follows:

1. The `uav_radio` module is imported along with other useful packages for computation.
2. A ROS node with the name `drone_rf_python_script` is initialized.
3. Two simple classes are implemented: `rf_body` for the radio path loss calculations, and `rf` for ROS setup, obtaining the location of the quadcopter, and printing the path loss to the terminal.
4. The constructor of `rf_body` class is responsible for creating an instance of the `uav_radio.PathLossCalculator` class

<sup>1</sup> ROS website: <https://www.ros.org/>

<sup>2</sup> *iq\_sim* GitHub: [https://github.com/Intelligent-Quads/iq\\_sim](https://github.com/Intelligent-Quads/iq_sim)

<sup>3</sup> Ardupilot website: <https://ardupilot.org/>

<sup>4</sup> Gazebo website: <https://gazebo.org/>

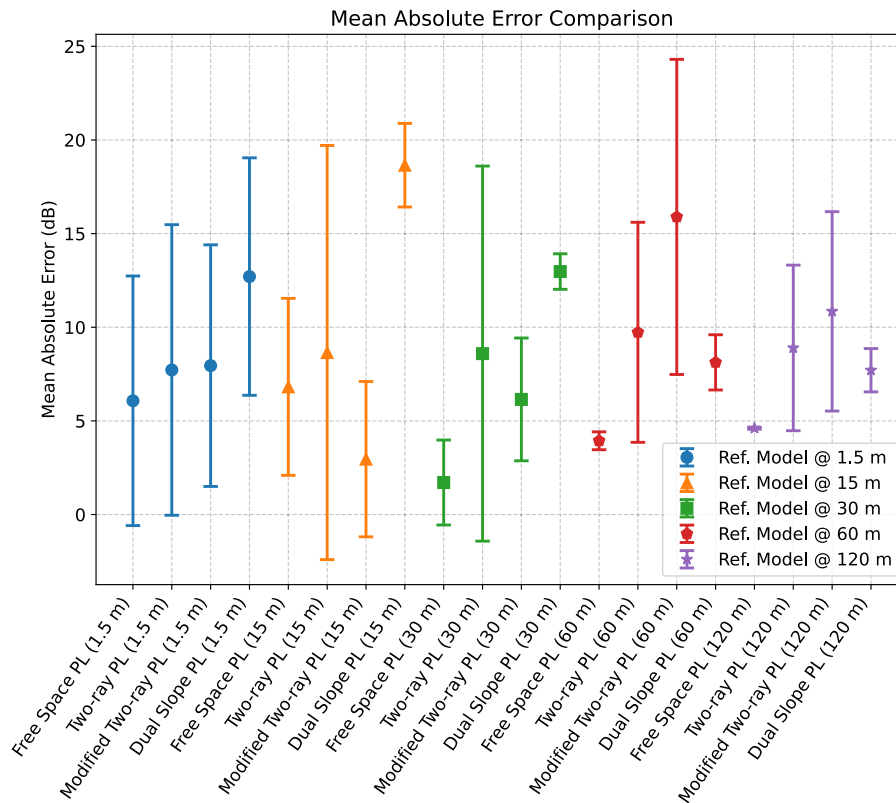


Fig. 5. Path Loss mean absolute error and standard deviation comparison at different heights between the fitted model from [12] and other available models.

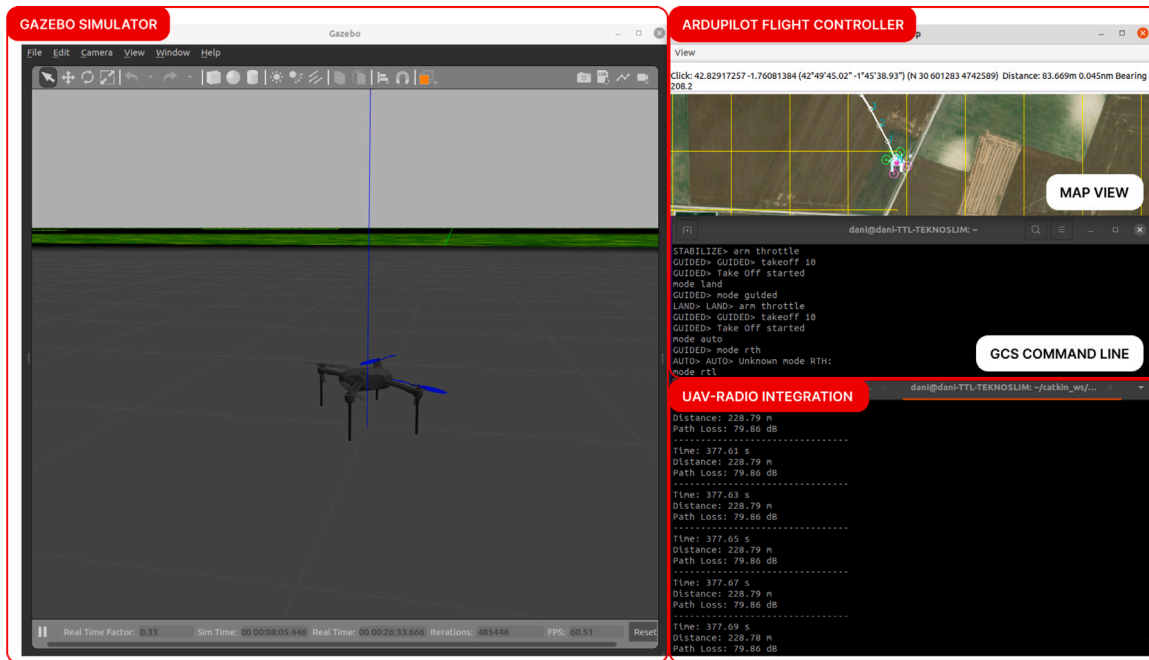


Fig. 6. Example setup featuring the Gazebo simulator, Ardupilot Flight Controller, iq\_sim’s multidrone environment, and the UAVRadio path loss estimation module.

with a reference distance of 1.0 m. The `get_distance_loss` method takes a distance parameter ( $d$ ) and calculates the PL using multiple frequencies and methods, such as `free_space_pl`, from the `PathLossCalculator`. The `calc_losses` method takes a position vector (`position`) and estimates the path loss based on the distance from the GCS to the quadcopter. It returns both the path loss and the distance.

5. The constructor of the `rf` class is used to setup the ROS position subscriber for the desired drone, and initialize the `rf_body` class. It also contains a `location_callback` method for continuously updating the position vector, and a `rf_signal` method that calls the `calc_losses` method from the `rf_body` instance to compute the path loss and print the calculated values.

When this code is run, it sets up a radio path loss calculation system for a quadcopter in a ROS-based simulation environment, calculates the PL due to spatial distance, and prints the results. It is designed for experimentation and testing in a simulated context. Using the additional methods included in this package, the results can easily be plotted in real-time, where different PL models can be used, and the frequency can be tuned to compare the performance of different radio frequencies under the specified conditions.

The flight consists of a straight-line mission in which the quadcopter moves away from the GCS, located at the origin, at a constant speed ( $v = 5$  m/s), and stops for 5 s at each waypoint located approximately every 30 m. The selected flight height has been 30 m. A short video demonstration of the provided example can be found in the Supplementary Material.<sup>5</sup>

For comparison purposes, this experiment has been run with five different PL models: the log-distance model, the log-distance alpha-beta model, the two-ray model, the modified two-ray model, and the dual slope model. The log-distance path loss model is configured for open-field settings due to mission characteristics. Transmitter and receiver heights have also been configured for the models where they are required. Three typical UAV frequencies have been selected for comparison: 868 MHz, 2.4 GHz, and 5.8 GHz.

After processing the PL estimated with each model on the straight-line flight mission, the results are compared in Fig. 7, where Figs. 7(a–c) present the comparison for the five selected models over time, for 868 MHz, 2.4 GHz and 5.8 GHz operating frequencies, respectively, and Figs. 7(d–f) depict the same results over distance. It can be observed from the figures that for all cases the PL has a trend of increasing losses with distance. Frequency also has a high impact, increasing the PL when higher frequencies are used. The Two-Ray Path Loss model, which considers the reflection on the ground in the scenario, presents higher variations, which is more realistic for this specific analyzed scenario. These variations are more frequent at the beginning of the flight, due to the vertical ascension of the UAV before starting the horizontal straight line mission. In the comparison of PL over time (Fig. 7 (up)), it is observed that the PL remains constant at some points. This is because at the time of designing the flight mission, the drone was set to hover for 5 s at each waypoint, which was approximately every 30 m distance.

#### 4. Impact

Signal propagation characteristics in UAV-related communication scenarios have a different behavior than cellular communication scenarios. They exhibit unique characteristics, in which the most important ones are the highly dynamic environment due to the velocity of the UAV, which induces non-stationary environments [3]. In this sense, signal propagation analysis in UAV communications scenarios has been disproportionately less addressed in the literature than cellular communications. Thus, it is necessary to consider accurate propagation models to estimate the received signal for these types of scenarios and communication links. In this regard, this package presents a significant impact in both research and engineering domains, offering valuable contributions in the field of UAVs and wireless communication systems, by facilitating path loss predictions in UAV-related wireless communication scenarios. Its adaptability, customization, and multi-scenario analysis capabilities make it an indispensable asset in advancing the field of UAV technology and wireless communication. Researchers and engineers can leverage this module to develop innovative solutions and improve the performance of UAV-based applications across various domains.

More specifically, this software is currently employed by our laboratory to simulate communication between the GCS and the UAV

in potentially hazardous scenarios. It can be easily integrated with a digital twin, to allow replication of experimental missions within the digital environment prior to conducting a real-world experiment, enabling the communication assessment without the associated risks.

#### 5. Conclusions

The UAVRadio Python module is a comprehensive toolkit designed to facilitate the analysis and prediction of radio signal path loss in UAV communication scenarios. The module comprises a range of path loss models referenced from established literature, offering users a powerful and flexible framework for estimating signal attenuation in different UAV communication links. This module includes a set of Python functions that allow considering the proper path loss model according to the scenario and UAV link analysis. In addition, the module offers a selection of multiple paths loss models, including free space, log-distance, two-ray, dual slope, or modified two-ray, among others.

Throughout this paper, we show how the module can be easily integrated with an open-source UAV digital twin to optimize UAV communication systems and ensure reliable wireless connectivity in a variety of operational scenarios. Using these additional methods, the results can be easily plotted in real-time, where different path loss models can be tested, and the frequency can be tuned to compare the performance of different setups under the specified conditions. We have also demonstrated a procedure to compare newly developed experimental models with the existing literature, which facilitates the investigation of new models in this field. From the presented examples, the importance of selecting an adequate channel model to estimate signal losses in UAV communications scenarios has been verified. The use of the presented library allows radio signal propagation analysis for UAV communications, in advance or in real-time, which could be a great aid when planning a mission.

The open-source package is readily available to engineers, researchers, and UAV enthusiasts for download, adaptation, and use in a wide range of projects. To enhance the usability of the software, comprehensive and up-to-date documentation is also provided.

#### CRedit authorship contribution statement

**Daniel Aláez:** Conceptualization, Investigation, Software, Validation, Writing – original draft, Writing – review & editing, Data curation, Visualization. **Mikel Celaya-Echarri:** Data curation, Formal analysis, Methodology, Project administration, Supervision, Writing – original draft, Writing – review & editing. **Leyre Azpilicueta:** Conceptualization, Data curation, Formal analysis, Methodology, Resources, Supervision, Writing – original draft, Writing – review & editing. **Jesús Villadangos:** Funding acquisition, Project administration, Resources, Supervision, Writing – review & editing.

#### Declaration of competing interest

The authors declare that they have no known competing financial interests or personal relationships that could have appeared to influence the work reported in this paper.

#### Data availability

Data will be made available on request.

#### Acknowledgments

This work was supported in part by Grant No. RYC2021-031949-I funded by MCIN/AEI/10.13039/501100011033 and NextGenerationEU/PRTR; in part by the Ministerio de Ciencia e Innovación (Spain) under the research grant CONDOR-Connected PID2021-127409OB-C31; and in part by the Government of Navarre (Departamento de Desarrollo Económico) under the research grant PC109-110 NAITEST. The authors have no competing interests to declare.

<sup>5</sup> Supplementary video example: <https://youtu.be/h9RS77cVn3A>



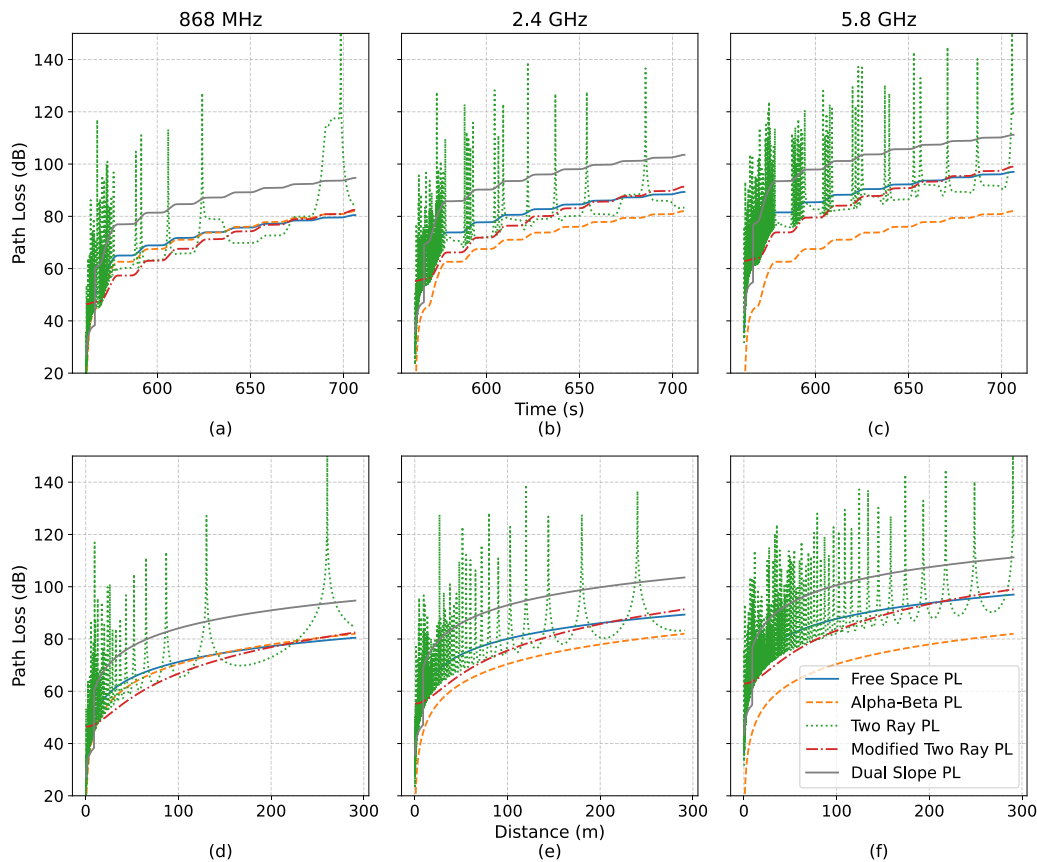


Fig. 7. Example comparison between five different PL models on a simulated straight line flight at 30 m height: PL versus time (up) and PL versus distance (down). Each column represents a different frequency setting: 868 MHz, 2.4 GHz, and 5.8 GHz.

## Appendix A. Supplementary data

Supplementary material related to this article can be found online at <https://doi.org/10.1016/j.softx.2023.101628>.

## References

- [1] Khawaja W, Guvenc I, Matolak DW, Fiebig U-C, Schneckenburger N. A survey of air-to-ground propagation channel modeling for unmanned aerial vehicles. *IEEE Commun Surv Tutor* 2019;21(3):2361–91.
- [2] Khuwaja AA, Chen Y, Zhao N, Alouini M-S, Dobbins P. A survey of channel modeling for UAV communications. *IEEE Commun Surv Tutor* 2018;20(4):2804–21.
- [3] Molisch AF. *Wireless communications: from fundamentals to beyond 5G*. John Wiley & Sons; 2023.
- [4] Zeng Y, Zhang R, Lim TJ. Wireless communications with unmanned aerial vehicles: opportunities and challenges. *IEEE Commun Mag* 2016;54(5):36–42.
- [5] Zeng Y, Wu Q, Zhang R. Accessing from the sky: A tutorial on UAV communications for 5G and beyond. *Proc IEEE* 2019;107(12):2327–75.
- [6] Li B, Fei Z, Zhang Y. UAV communications for 5G and beyond: Recent advances and future trends. *IEEE Internet Things J* 2019;6(2):2241–63.
- [7] Zeng Y, Lyu J, Zhang R. Cellular-connected UAV: Potential, challenges, and promising technologies. *IEEE Wirel Commun* 2019;26(1):120–7.
- [8] Mozaffari M, Saad W, Bennis M, Nam Y-H, Debbah M. A tutorial on UAVs for wireless networks: Applications, challenges, and open problems. *IEEE Commun Surv Tutor* 2019;21(3):2334–60.
- [9] Khan SK, Naseem U, Siraj H, Razzak I, Imran M. The role of unmanned aerial vehicles and mmWave in 5G: Recent advances and challenges. *Trans Emerg Telecommun Technol* 2021;32(7):1–18.
- [10] Xiao Z, Zhu L, Liu Y, Yi P, Zhang R, Xia X-G, et al. A survey on millimeter-wave beamforming enabled UAV communications and networking. *IEEE Commun Surv Tutor* 2022;24(1):557–610.
- [11] Rappaport T, Heath R, Daniels R, Murdock J. *Millimeter wave wireless communications*. Prentice Hall; 2015.
- [12] Amorim R, Nguyen H, Mogensen P, Kovács IZ, Wigard J, Sørensen TB. Radio channel modeling for UAV communication over cellular networks. *IEEE Wirel Commun Lett* 2017;6(4):514–7.
- [13] Yanmaz E, Kuschnig R, Bettstetter C. Achieving air-ground communications in 802.11 networks with three-dimensional aerial mobility. In: 2013 Proceedings IEEE INFOCOM. IEEE; 2013, p. 120–4.
- [14] Newhall WG, Mostafa R, Dietrich C, Anderson CR, Dietze K, Joshi G, et al. Wideband air-to-ground radio channel measurements using an antenna array at 2 GHz for low-altitude operations. In: IEEE military communications conference, 2003., vol. 2. IEEE; 2003, p. 1422–7.
- [15] Matolak DW, Sun R. Air-ground channel characterization for unmanned aircraft systems—Part III: The suburban and near-urban environments. *IEEE Trans Veh Technol* 2017;66(8):6607–18.
- [16] Khawaja W, Guvenc I, Matolak D. UWB channel sounding and modeling for UAV air-to-ground propagation channels. In: 2016 IEEE global communications conference. IEEE; 2016, p. 1–7.
- [17] Sun R, Matolak DW. Air-ground channel characterization for unmanned aircraft systems part II: Hilly and mountainous settings. *IEEE Trans Veh Technol* 2016;66(3):1913–25.
- [18] Matolak DW, Sun R. Air-ground channel characterization for unmanned aircraft systems—Part I: Methods, measurements, and models for over-water settings. *IEEE Trans Veh Technol* 2016;66(1):26–44.
- [19] Cai X, Gonzalez-Plaza A, Alonso D, Zhang L, Rodríguez CB, Yuste AP, et al. Low altitude UAV propagation channel modelling. In: 2017 11th European conference on antennas and propagation. IEEE; 2017, p. 1443–7.
- [20] Goddemeier N, Daniel K, Wietfeld C. Role-based connectivity management with realistic air-to-ground channels for cooperative UAVs. *IEEE J Sel Areas Commun* 2012;30(5):951–63.